56. Muon Anomalous Magnetic Moment

Revised August 2025 by D.W. Hertzog (U. Washington) and M. Hoferichter (U. Bern).

56.1 Introduction and summary

The Dirac equation predicts a muon magnetic moment, $\boldsymbol{\mu} = g_\mu \frac{q}{2m_\mu}\mathbf{S}$, with gyromagnetic ratio $g_\mu = 2$, charge q, and mass m_μ. Quantum loop effects lead to a small calculable deviation from $g_\mu = 2$, parameterized by the anomalous magnetic moment of the muon $a_\mu \equiv (g_\mu - 2)/2$. This observable can be measured in storage-ring experiments and predicted within the Standard Model (SM) to high precision, testing the SM at its quantum loop level. In short, the current world average of the experimental determination after the final results of the FNAL E989 experiment reads [1–8]

$$a_\mu^{\rm exp} = 116\,592\,071.5(14.5) \times 10^{-11}\,, \tag{56.1}$$

to be compared with the SM prediction as compiled by the Muon $g-2$ Theory Initiative [9–69]

$$a_\mu^{\rm SM} = 116\,592\,033(62) \times 10^{-11}\,. \tag{56.2}$$

Accordingly, the difference

$$\Delta a_\mu \equiv a_\mu^{\rm exp} - a_\mu^{\rm SM} = 38(63) \times 10^{-11} \tag{56.3}$$

is compatible with zero, but the uncertainty is completely dominated by the SM prediction, allowing for a SM test at three-fold improved precision once the experimental uncertainty can be matched. In Sec. 56.2 we briefly review the status of experiment, Eq. (56.1), in Sec. 56.3 the status of the SM prediction, Eq. (56.2), and conclude with some remarks on future improvements in Sec. 56.4.

56.2 Precision measurement of a_μ

The two most precise muon $g-2$ experiments—BNL E821 and FNAL E989—were developed based on the experiences of earlier storage ring experiments at CERN [70,71]. The most significant improvements are related to the intensity and purity of muon delivery to the ring, which has led to the world average precision of 124 ppb in the determination of a_μ. Figure 56.1 displays the consistency of the individual BNL and FNAL run-period publications,[1] the final precision achieved, and the average. With the exception of BNL-01, all measurements used positive muons. Details of the combination procedure, including updated corrections since the original publication, can be found in Ref. [1].

In this compact description, we emphasize aspects of the common storage ring technique to determine a_μ to high precision, while also pointing out the relatively balanced final systematics table from FNAL that would have to be overcome for further improvements.

Polarized muon bunches are injected into a 7.1 m radius superconducting storage ring (SR) [76] having a highly uniform vertical magnetic field, $|\mathbf{B}| \approx 1.45$ T. A fast kicker magnet [77] deflects the muons during the first turn into a fiducial toroidal volume that is concentric with the SR center. Four regions containing electrostatic quadrupole (ESQ) plates provide weak vertical focusing. Approximately 5000 muons are stored in each "fill" of the ring.

The muons circulate in the ring at the cyclotron angular frequency $\boldsymbol{\omega}_c = -\frac{q}{m_\mu\gamma}\mathbf{B}$, $\gamma = 1/\sqrt{1-\beta^2}$ being the Lorentz factor, and their spins rotate at $\boldsymbol{\omega}_s = -g_\mu \frac{q}{2m_\mu}\mathbf{B} - (1-\gamma)\frac{q}{m_\mu\gamma}\mathbf{B}$. If g_μ were exactly equal to 2, the cyclotron and spin frequencies would be the same. For $g_\mu \neq 2$,

[1] The quoted BNL $\mathcal{R}'_\mu$ and a_μ values were computed by the FNAL Muon $g-2$ collaboration [1], converting the reported values for free protons in vacuum in the BNL references and using the converted $\mathcal{R}'_\mu$ values to re-compute the a_μ values relying on CODATA 2022 [75] for the external inputs.

Figure 56.1: Experimental values of a_μ from BNL E821 (blue triangles) [72–74],[1] FNAL E989 (red squares) [1,2,4], and the world average (black diamond). The uncertainties combine statistics and systematics. BNL values are rounded to the nearest 10 ppb. All measurements employed positive muons except BNL-01, which ran with negative muons (inverted triangle).

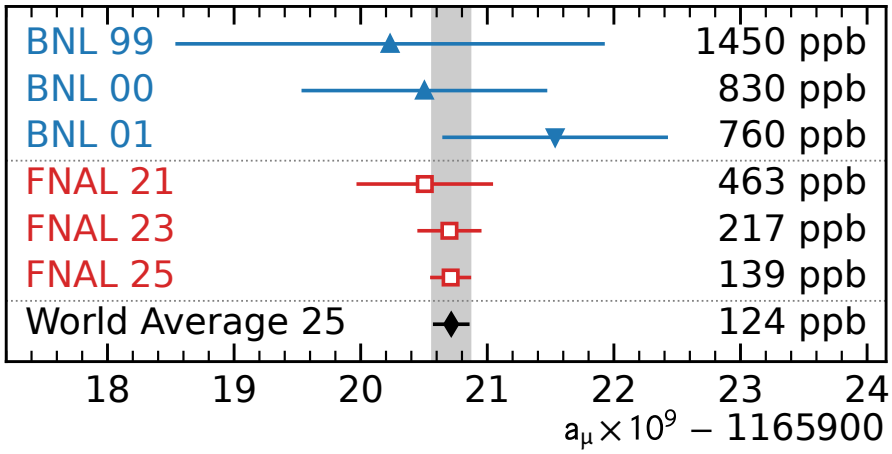

and for the ideal case that $\boldsymbol{\beta} \cdot \mathbf{B} = 0$, the anomalous precession frequency $\boldsymbol{\omega}_a$ is simply given by

$$\boldsymbol{\omega}_a = \boldsymbol{\omega}_s - \boldsymbol{\omega}_c = -\frac{q}{m_\mu} a_\mu \mathbf{B}. \tag{56.4}$$

In practice, the betatron oscillations of the muon beam and the presence of the quadrupole electric field lead to a more complete expression [78]

$$\boldsymbol{\omega}_a = -\frac{q}{m_\mu}\left[a_\mu \mathbf{B} - a_\mu\left(\frac{\gamma}{\gamma+1}\right)(\boldsymbol{\beta}\cdot\mathbf{B})\boldsymbol{\beta} - \left(a_\mu - \frac{1}{\gamma^2-1}\right)\boldsymbol{\beta}\times\mathbf{E}\right]. \tag{56.5}$$

The second term accounts for the vertical betatron oscillations owing to the average value of $(\boldsymbol{\beta}\cdot\mathbf{B})^2$. A measurement of the vertical amplitude distribution leads to a "pitch" correction. The third term accounts for the motional magnetic field felt by the relativistic muons in the presence of the ESQ electric field $\mathbf{E}$. The CERN-III experiment [71] recognized that this term vanishes for $\gamma = \sqrt{1+1/a_\mu} \approx 29.3$, corresponding to a muon "magic momentum" of $P_0 \approx 3.094\,\text{GeV}$.[2] The CERN-III, BNL, and FNAL experiments each operated at this momentum. The momentum spread with respect to P_0 ($\sim \Delta P/P_0 < 0.2\%$) requires an electric-field correction of order several hundred ppb, by far the largest correction in the experiment.

The magnetic field $\mathbf{B}$ in Eq. (56.5) is measured using pulsed proton NMR techniques and is expressed as $\tilde{\omega}'_p(T_r)$, which is the proton spin precession frequency inside a room-temperature spherical water sample and averaged over the stored muon distribution. Equation (56.5) demonstrates that $a_\mu \propto \omega_a/\tilde{\omega}'_p(T_r) \equiv \mathcal{R}'_\mu$, which is the quantity reported by all $g-2$ experiments. The muon anomaly is then determined from

$$a_\mu = \mathcal{R}'_\mu \frac{\mu'_p(T_r)}{\mu_B}\frac{m_\mu}{m_e}, \tag{56.6}$$

[2] The E34 experiment at J-PARC [79] plans to inject lower momentum muons with negligible transverse momentum components into a ring that does not include an electric quadrupole field. This will greatly reduce any needed electric field or pitch correction.

Table 56.1: $\mathcal{R}'_\mu$ values and uncertainties from BNL E821,[1] with uncertainties rounded to the nearest 10 ppb, and those from FNAL E989.

	$\mathcal{R}'_\mu$	Total (ppb)	Statistical (ppb)	Systematics (ppb)
BNL E821	0.00370730154	540 ppb	460	280
FNAL E989	0.00370730088	125 ppb	98	78
Combined	0.00370730091	122 ppb	96	75

Table 56.2: Corrections and uncertainties from combined FNAL running periods, and current uncertainties due to the external parameters. Here ω_a^m is the fit precession frequency. Corrections to ω_a^m yield ω_a, needed in the numerator of $\mathcal{R}'_\mu$. Numerical summary courtesy of Alberto Lusiani, on behalf of the FNAL Muon $g-2$ Collaboration.

Quantity	Correction (ppb)	Uncertainty (ppb)
ω_a^m (statistical)	–	98
Beam dynamic (BD) corrections to ω_a^m to yield ω_a	+538	43
Net ω_a (statistical + BD + fitting uncertainties)	–	111
ω'_p (all systematics)	–	48
Magnetic field transient corrections to ω'_p	−58	31
Net ω'_p uncertainty	–	57
Total uncertainties for $\mathcal{R}'_\mu$	–	125
μ'_p/μ_B and m_μ/m_e external parameters	–	23
Total for a_μ		127

where $\mu'_p(T_r)/\mu_B$ is the ratio of the shielded proton magnetic moment to the Bohr magneton and m_μ/m_e is the muon-to-electron mass ratio [75]. Reporting this ratio allows a_μ to be recalculated if the fundamental constants are updated; see Table 56.1.

The absolute magnetic field [6] is established using custom high-purity water [80] and He-3 [81] probes measured in a special-purpose highly uniform MRI magnet. These probes cross-calibrate an in-ring movable "plunging" probe system, which in turn cross-calibrates one-by-one the 17 probes in an NMR trolley [82]. This device periodically maps the entire storage ring field *in situ*. The temporal variation of the field is continuously monitored using an additional set of 378 probes [83] placed above and below the fiducial volume.

Two arrays of in-vacuum straw Tracker detectors [84] located at two azimuthal positions in the SR record the inward bending trajectories of e^+ from muon decay. The fit tracks are then traced back to the approximate upstream decay location within the storage ring vs. time-in-fill. The measured stored muon distribution is folded with the azimuthally averaged field maps to give the muon-weighted field. Details are found in Refs. [3, 6].

Parity violation in weak $\mu^+ \to e^+\nu_e\bar{\nu}_\mu$ decay provides the polarimetry needed to deduce the average muon spin direction vs. time-in-fill. The decay positron energy in the boosted laboratory frame is related to the energy and angular distribution in the center-of-mass (CM) as in $E_{e,\mathrm{lab}} \approx \gamma E_{e,\mathrm{CM}}(1+\cos\theta_{\mathrm{CM}})$, and thus the highest-energy positrons are preferentially emitted in the direction of the muon spin. All decay positrons curl to the inside of the SR, where their time-of-arrival and energy are measured in calorimeters [85], forming a measured spectrum $N(t, E_e)$. In

Figure 56.2: Sample diagrams for a_μ in the SM: solid lines refer to the muon, wiggly lines to photons, and the red blobs to hadronic matrix elements. The first diagram gives the leading QED contribution by Schwinger, the second one represents a one-loop EW diagram with Z exchange, and the last two diagrams correspond to HVP and HLbL topologies, respectively.

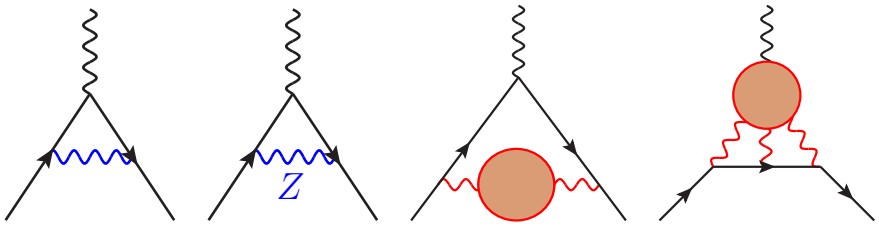

first order, this spectrum can be described by $N(t) = N_0 e^{-t/(\gamma\tau_\mu)}[1 + A\cos(\omega_a t - \phi)]$, where the asymmetry A depends on the energy threshold and the average polarization of the muons. The statistical precision of the experiment is optimized by fitting a histogram whose entries are weighted by the energy-dependent asymmetry $A(E)$; that is,

$$\frac{\delta\omega_a}{\omega_a} = \frac{1}{\omega_a\gamma\tau_\mu}\sqrt{\frac{2}{N\langle A(E)^2\rangle}}\,, \tag{56.7}$$

which emphasizes the importance of the higher-energy positrons.

The fit of $N(t, E_e)$ results in the measured precession frequency ω_a^m. To achieve a good χ^2, additional terms that account for the rate variations from the coupling of calorimeter acceptance to beam motions are required. The largest of these are associated with coherent betatron oscillations (CBO), which, if ignored, would pull ω_a^m from the true precession frequency ω_a by several hundred ppb. An RF modulation system [86], tuned to the CBO frequency and applied to the ESQ plates, creates a dipole field that significantly damps the intrinsic CBO effect. Details on the extraction of ω_a^m and the many independent checks and methods used can be found in Refs. [3, 5].

Table 56.2 lists the corrections and uncertainties reported for the entire FNAL E989 measurement [1, 2, 4]. For simplicity, this table combines the individual effects that impact ω_a^m or ω_p'. Corrections to the measured precession frequency, ω_a^m, are dominated by the effect of the electric field and pitch as expressed in Eq. (56.5). Several additional and much smaller corrections are needed because the stored muon phase space slightly evolves during the fill. Transient-magnetic-field corrections to ω_p' correspond to a residual eddy current from the fast kicker and a vibration-induced field perturbation from the charging of the ESQ plates. The systematic uncertainties are relatively balanced. The final precision on $\mathcal{R}_\mu'$, and thus also on a_μ, is dominated by the statistical uncertainty.

56.3 Standard Model prediction of a_μ

The SM prediction of a_μ decomposes into pure QED contributions, electroweak (EW) effects, and hadronic corrections

$$a_\mu^{\rm SM} = a_\mu^{\rm QED} + a_\mu^{\rm EW} + a_\mu^{\rm had}\,, \qquad a_\mu^{\rm had} = a_\mu^{\rm HVP} + a_\mu^{\rm HLbL}\,, \tag{56.8}$$

where the latter are further separated into topologies featuring hadronic vacuum polarization (HVP) and hadronic light-by-light scattering (HLbL), see Fig. 56.2 for representative diagrams in each category. In the subsequent sections we briefly discuss the status for each class of corrections,

Table 56.3: Summary of all contributions to the SM prediction and comparison to experiment, adapted from Ref. [9].

Contribution	Value $\times 10^{11}$	References
Experiment (E989, E821)	116 592 071.5(14.5)	Refs. [1–8]
HVP LO (lattice)	7132(61)	Refs. [21–37]
HVP LO (e^+e^-, τ)	Estimates not provided at this point	
HVP NLO (e^+e^-)	−99.6(1.3)	Refs. [38, 39]
HVP NNLO (e^+e^-)	12.4(1)	Ref. [40]
HLbL (phenomenology)	103.3(8.8)	Refs. [19, 41–63]
HLbL NLO (phenomenology)	2.6(6)	Ref. [64]
HLbL (lattice)	122.5(9.0)	Refs. [65–69]
HLbL (phenomenology + lattice)	112.6(9.6)	Refs. [19, 41–63, 65–69]
QED	116 584 718.8(2)	Refs. [10–16]
EW	154.4(4)	Refs. [17–20]
HVP LO (lattice) + HVP N(N)LO (e^+e^-)	7045(61)	Refs. [21–40]
HLbL (phenomenology + lattice + NLO)	115.5(9.9)	Refs. [19, 41–69]
Total SM Value	116 592 033(62)	Refs. [10–69]
Difference: $\Delta a_\mu \equiv a_\mu^{\rm exp} - a_\mu^{\rm SM}$	38(63)	

referring to Refs. [9, 87] for a thorough review, labeled as WP20 [87] and WP25 [9] below.[3] The resulting bottom line is summarized in Table 56.3.

56.3.1 *QED and electroweak contributions*

By far the dominant contribution to $a_\mu^{\rm SM}$ arises from QED, including all diagrams with purely photonic and leptonic ($\ell = e, \mu, \tau$) loops. Starting from Schwinger's seminal result [89], the expansion can be expressed as

$$a_\mu^{\rm QED} = \frac{\alpha}{2\pi} + 0.765\,857\,420(8)_e(11)_\tau[13]\left(\frac{\alpha}{\pi}\right)^2 + 24.050\,509\,77(17)_e(16)_\tau[23]\left(\frac{\alpha}{\pi}\right)^3 + 130.8782(60)_{\rm MC}\left(\frac{\alpha}{\pi}\right)^4 + 750.2(9)_{\rm MC}\left(\frac{\alpha}{\pi}\right)^5 + \mathcal{O}(\alpha^6)\,, \tag{56.9}$$

where the uncertainties derive from $m_\mu/m_e = 206.7682827(46)$, $m_\tau/m_\mu = 16.8170(11)$ [75], and Monte-Carlo (MC) integration, respectively. Up to $\mathcal{O}(\alpha^3)$, analytical results are available, both for the mass-independent terms [90–92] and mass-dependent corrections [93–95], so that the uncertainties in the coefficients in Eq. (56.9) only depend on the input for the lepton mass ratios. At $\mathcal{O}(\alpha^4)$, the mass-independent term is known essentially analytically [96], and the uncertainty in the mass-dependent corrections is dominated by MC errors [10, 97]. Finally, at $\mathcal{O}(\alpha^5)$ both mass-independent and mass-dependent contributions are evaluated numerically, and the size of the mass-independent term recently decreased by $\simeq 0.8$ upon improved MC sampling [10–13], about the same size as the MC uncertainty in the mass-dependent correction. Numerically, the largest contributions to the coefficients arise from terms enhanced by powers of $\log \frac{m_\mu}{m_e}$ (and factors of π^2), explaining their rapid increase. For the evaluation of $a_\mu^{\rm QED}$, input for the fine-structure constant α

[3] These white papers (WP) were compiled by the Muon $g-2$ Theory Initiative [88], reflecting a community consensus of the status of the SM prediction in 2020 and 2025, respectively.

is required, the current most precise determinations being [9]

$$\alpha^{-1}[\mathrm{Cs}] = 137.035\,999\,045(27)\,, \tag{56.10}$$

$$\alpha^{-1}[\mathrm{Rb}] = 137.035\,999\,2052(97)\,, \tag{56.11}$$

$$\alpha^{-1}[a_e] = 137.035\,999\,163(15)\,, \tag{56.12}$$

derived from atom-interferometry measurements in Cs [14], Rb [15], and the anomalous magnetic moment of the electron a_e [16], respectively. α^{-1}[Cs] and α^{-1}[Rb] disagree by 5.5σ, which translates to an uncertainty of about 0.14×10^{-11} in a_μ^{QED}. This is the same level at which $\mathcal{O}(\alpha^6)$ contributions are expected to enter, estimated based on the maximally possible enhancement with $\log\frac{m_\mu}{m_e}$ at six-loop order [10]. The combination of these two effects leads to the final uncertainty quoted for a_μ^{QED} in Table 56.3.

Loop contributions that involve W, Z, or Higgs bosons are summarized in the EW contribution a_μ^{EW}. At one-loop order, the result can be expressed as [98–102]

$$a_\mu^{\mathrm{EW}}[\text{1-loop}] = \frac{G_F}{\sqrt{2}}\frac{m_\mu^2}{8\pi^2}\left[\frac{5}{3}+\frac{1}{3}(1-4s_{\mathrm{W}}^2)^2+\mathcal{O}\left(\frac{m_\mu^2}{M_W^2},\frac{m_\mu^2}{M_H^2}\right)\right] = 194.79(1)\times10^{-11}\,, \tag{56.13}$$

with on-shell weak mixing angle $s_W^2 = \sin^2\theta_W = 1 - M_W^2/M_Z^2$ and the SM prediction expressed in terms of the Fermi constant G_F as measured in muon decay [103], M_Z, and α, while M_W is a derived quantity [18]. Two-loop contributions are sizable, $a_\mu^{\mathrm{EW}}[\text{2-loop}] = -40.4(4)\times10^{-11}$, and are typically further separated into bosonic [104–106], Higgs-dependent [18, 107], and other fermionic contributions [17, 108, 109]. In particular, the latter include quark triangle loops, for which non-perturbative effects become important. Improvements in their evaluation [19, 20] together with the consideration of α_s corrections for the heavy quarks [110] and lattice-QCD input for γ–Z mixing [111] lead to the updated result [20]

$$a_\mu^{\mathrm{EW}} = 154.4(4)\times10^{-11}\,, \tag{56.14}$$

where three-loop effects are estimated to be $\lesssim 0.2\times10^{-11}$ [17, 112].

56.3.2 *Hadronic light-by-light scattering*

HLbL contributions enter at $\mathcal{O}(\alpha^3)$, involving the hadronic four-point function as indicated in Fig. 56.2, which can be determined with data-driven techniques or using lattice QCD. For a detailed review we refer to Ref. [9], while a summary of the present situation is shown in Fig. 56.3. Phenomenological [19, 41–63] and lattice-QCD [65–69] evaluations agree at a level of 1.5σ, leading to the overall average

$$a_\mu^{\mathrm{HLbL}}[\text{phenomenology + lattice}] = 112.6(9.6)\times10^{-11}\,, \tag{56.15}$$

whose error includes a scale factor $S = 1.5$. Including an estimate for NLO HLbL topologies [64] then produces the final HLbL number quoted in Table 56.3.

56.3.3 *Hadronic vacuum polarization*

The leading, and most critical, hadronic effect already arises at $\mathcal{O}(\alpha^2)$ in the form of the HVP diagram shown in Fig. 56.2. Traditionally, this contribution has been evaluated using the master formula [114, 115]

$$a_\mu^{\mathrm{HVP,\,LO}} = \left(\frac{\alpha m_\mu}{3\pi}\right)^2\int_{s_{\mathrm{thr}}}^{\infty} ds\frac{\hat{K}(s)}{s^2}R_{\mathrm{had}}(s)\,, \tag{56.16}$$

Figure 56.3: Summary of HLbL evaluations, from data-driven methods (green), lattice QCD (blue), and combinations (black). The averages are from WP20 and WP25, respectively, the other points refer to HSZ-24 [61,113], RBC/UKQCD-19 [65], Mainz/CLS-21+22 [66,67], RBC/UKQCD-23 [68], and BMW-24 [69]. Adapted from Ref. [9].

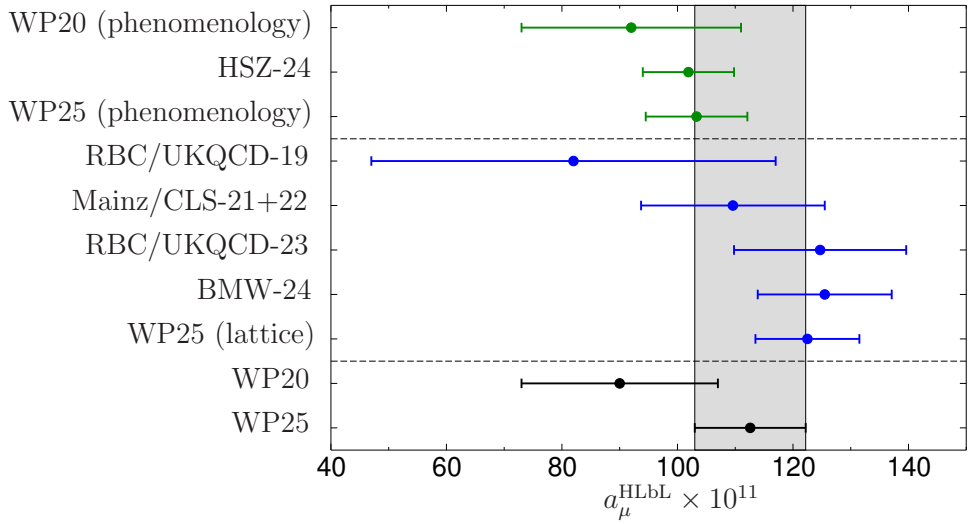

which allows one to express its effect via a dispersion integral in terms of the hadronic R-ratio,

$$R_{\rm had}(s) = \frac{3s}{4\pi\alpha^2}\sigma\left[e^+e^- \to \text{hadrons}(+\gamma)\right], \tag{56.17}$$

and a kernel function $\hat{K}(s)$. In particular, the LO contribution is defined photon-inclusively, but removing vacuum-polarization effects in the photon propagator. Accordingly, the integration starts at the threshold of the $e^+e^- \to \pi^0\gamma$ channel, $s_{\rm thr} = M_{\pi^0}^2$. In WP20, the final result for the HVP contribution was based on e^+e^- data, including data for the by far numerically dominant $e^+e^- \to \pi^+\pi^-$ channel from the SND06 [116], CMD-2 [117], BaBar [118], KLOE [119], and BESIII [120] experiments. Moreover, different methodologies for the compilation of e^+e^- data were taken into account [38, 121–125], and an additional uncertainty beyond a simple scale factor was introduced to account for the tension between the BaBar and KLOE measurements, leading to the gray band in Fig. 56.4.

Subsequently, new $\pi^+\pi^-$ measurements from SND20 [131] and CMD-3 [132,133] have become available, and while the former falls within the previous range, the latter increases tensions to a level that cannot be taken into account anymore by a meaningful inflation of uncertainties. For that reason, e^+e^- data are not used in WP25 for the LO HVP evaluation at this point, until the origin of the discrepancies among data sets is understood.[4]

An alternative data-driven evaluation relies on $\tau \to \nu_\tau$ + hadrons decays [136], in which case isospin symmetry provides access to the isovector part of the hadronic cross section as long as isospin-breaking corrections [137–142] can be controlled. A critical review of these corrections is provided in WP25, identifying several effects that currently preclude the use of τ data for the HVP evaluation due to a remaining model dependence that is difficult to quantify in a reliable manner. However, the current best estimate from WP25 (based on Refs. [126,129,140,142,143]) is included in the second panel of Fig. 56.4.

[4]The exception concerns higher-order HVP iterations [40,134], for which the increased uncertainty can be tolerated [38,39]. Mixed leptonic and hadronic corrections at $\mathcal{O}(\alpha^4)$ are $\lesssim 1 \times 10^{-11}$ [135].

Figure 56.4: Summary of various determinations of $a_\mu^{\mathrm{HVP,\,LO}}$, propagated to a_μ^{SM}. The first two panels refer to data-driven determinations, where the three points for each e^+e^- experiment reflect the CHKLS [123, 126–128] (triangle), DHMZ [121, 125, 129] (diamond), and KNTW [38, 122, 130] (square) methods, see WP25 for details. The gray band indicates the WP20 result, based on the e^+e^- experiments above the first dashed line. The second panel represents e^+e^- experiments that became available afterwards as well as the τ-based estimate from WP25. The last panel summarizes lattice-QCD determinations, including the hybrid evaluation by BMW/DMZ-24 [31], three individual lattice-QCD calculations by RBC/UKQCD-24+18 [33], Mainz/CLS-24 [34], BMW-20 [23], and five lattice HVP averages from WP25. The blue band refers to the final WP25 result, which coincides with "Avg. 1." In all cases, except for the gray WP20 band, the remaining contributions to a_μ^{SM} beyond $a_\mu^{\mathrm{HVP,\,LO}}$ are taken from WP25. The red band denotes the experimental world average. Adapted from Ref. [9].

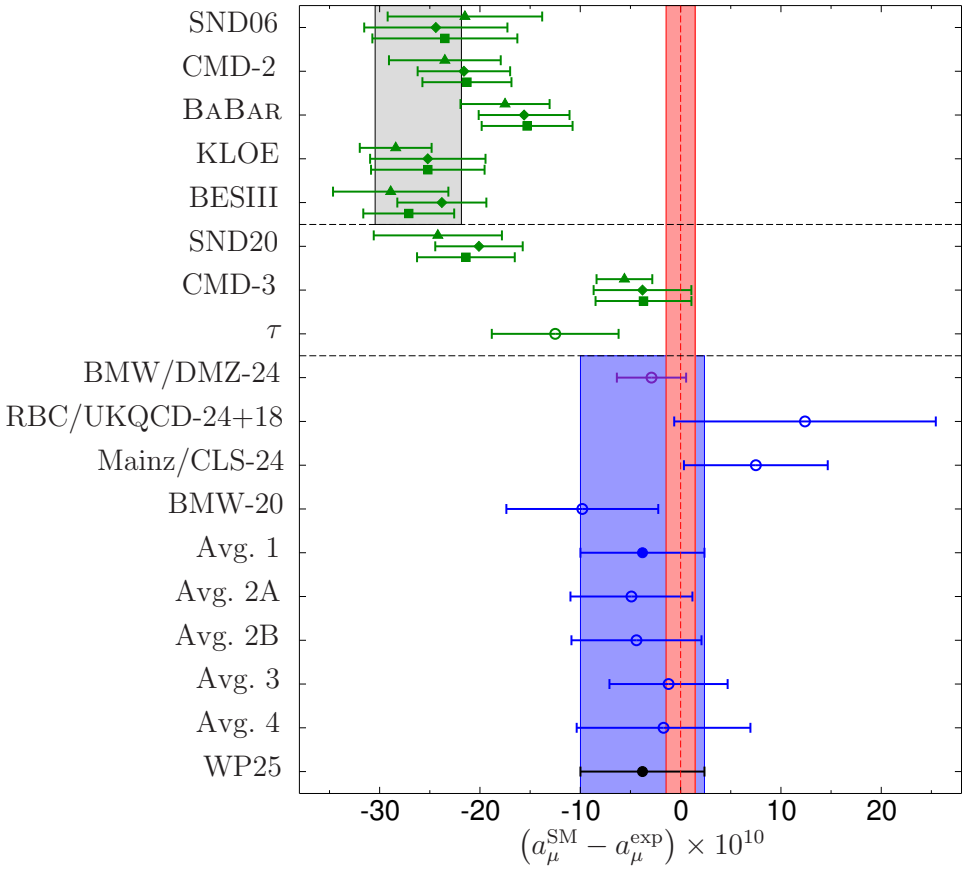

While the HVP evaluation from data-driven methods is thus inconclusive at this point, material progress has been achieved since WP20 in lattice QCD, based on the time-momentum representation of the hadronic two-point function [144]. In particular, detailed cross checks have been performed using windows in Euclidean time [21] as a tool to scrutinize the different systematic errors of the calculation. In total, the final average quoted in WP25,

$$a_\mu^{\mathrm{HVP,\,LO}}[\mathrm{lattice}] = 7132(61) \times 10^{-11}\,, \tag{56.18}$$

is based on 17 different papers from 8 independent lattice-QCD collaborations [21–37], from which three almost complete lattice calculations of the entire LO HVP contribution are derived [23,33,34],

see Fig. 56.4. Moreover, different strategies to combine the individual results (corresponding to the five averages shown in Fig. 56.4) prove very stable, and additional systematic errors have been assigned to cover the most challenging aspects of the calculation related to the evaluation of isospin-breaking effects and the noisy contributions at long distances. Given this consolidation of lattice-QCD results, the final SM prediction in WP25, as reproduced in Table 56.3, is based on Eq. (56.18),[5] until the tensions among the data-driven evaluations are resolved.

56.4 Outlook

In the current situation, it is obvious that the SM prediction (56.2) needs to be improved by a factor of four to fully leverage the precision achieved in experiment (56.1), which would result in a three-fold improved precision of the SM test (56.3). Ongoing efforts include [145]:

- Data-driven and lattice-QCD evaluations of the HLbL contribution will be further scrutinized to better understand their slight tension and hopefully further improve the precision.
- Lattice-QCD calculations will be performed at increased precision, with focus on more precise evaluations of isospin-breaking effects and the noisy contributions at long distances.
- New e^+e^- results are expected from BaBar, KLOE (existing data that were never analyzed before) and Belle II, BESIII, SND (new data). In addition, the role of radiative corrections and MC generators will be carefully scrutinized [146–152].
- New data for τ decays are expected from Belle II, and improved determinations of the required isospin-breaking corrections will be developed using lattice QCD, dispersion relations, and data-driven techniques.
- An independent direct measurement of a_μ is the goal of the E34 experiment at J-PARC [79].
- The MUonE experiment [153–155] aims at a measurement of the HVP contribution in a spacelike process, yielding another independent determination with completely different systematics.

References

[1] D. P. Aguillard *et al.* (Muon $g-2$), Phys. Rev. Lett. **135**, 10, 101802 (2025), [arXiv:2506.03069].

[2] D. P. Aguillard *et al.* (Muon $g-2$), Phys. Rev. Lett. **131**, 16, 161802 (2023), [arXiv:2308.06230].

[3] D. P. Aguillard *et al.* (Muon $g-2$), Phys. Rev. D **110**, 3, 032009 (2024), [arXiv:2402.15410].

[4] B. Abi *et al.* (Muon $g-2$), Phys. Rev. Lett. **126**, 14, 141801 (2021), [arXiv:2104.03281].

[5] T. Albahri *et al.* (Muon $g-2$), Phys. Rev. D **103**, 7, 072002 (2021), [arXiv:2104.03247].

[6] T. Albahri *et al.* (Muon $g-2$), Phys. Rev. A **103**, 4, 042208 (2021), [arXiv:2104.03201].

[7] T. Albahri *et al.* (Muon $g-2$), Phys. Rev. Accel. Beams **24**, 4, 044002 (2021), [arXiv:2104.03240].

[8] G. W. Bennett *et al.* (Muon $g-2$), Phys. Rev. D **73**, 072003 (2006), [hep-ex/0602035].

[9] R. Aliberti *et al.*, Phys. Rept. **1143**, 1 (2025), [arXiv:2505.21476].

[10] T. Aoyama *et al.*, Phys. Rev. Lett. **109**, 111808 (2012), [arXiv:1205.5370].

[11] S. Volkov, Phys. Rev. D **100**, 9, 096004 (2019), [arXiv:1909.08015].

[12] S. Volkov, Phys. Rev. D **110**, 3, 036001 (2024), [arXiv:2404.00649].

[13] T. Aoyama *et al.*, Phys. Rev. D **111**, 3, L031902 (2025), [arXiv:2412.06473].

[14] R. H. Parker *et al.*, Science **360**, 191 (2018), [arXiv:1812.04130].

[5] This result agrees with the hybrid evaluation by BMW/DMZ-24 [31], using data input for the long-distance tail.

[15] L. Morel *et al.*, Nature **588**, 7836, 61 (2020).

[16] X. Fan *et al.*, Phys. Rev. Lett. **130**, 7, 071801 (2023), [arXiv:2209.13084].

[17] A. Czarnecki, W. J. Marciano and A. Vainshtein, Phys. Rev. D **67**, 073006 (2003), [Erratum: Phys. Rev. D **73**, 119901 (2006)], [hep-ph/0212229].

[18] C. Gnendiger, D. Stöckinger and H. Stöckinger-Kim, Phys. Rev. D **88**, 053005 (2013), [arXiv:1306.5546].

[19] J. Lüdtke, M. Procura and P. Stoffer, JHEP **04**, 130 (2025), [arXiv:2410.11946].

[20] M. Hoferichter *et al.*, Phys. Rev. Lett. **134**, 20, 201801 (2025), [arXiv:2503.04883].

[21] T. Blum *et al.* (RBC, UKQCD), Phys. Rev. Lett. **121**, 2, 022003 (2018), [arXiv:1801.07224].

[22] D. Giusti *et al.* (ETM), Phys. Rev. D **99**, 11, 114502 (2019), [arXiv:1901.10462].

[23] S. Borsányi *et al.*, Nature **593**, 7857, 51 (2021), [arXiv:2002.12347].

[24] C. Lehner and A. S. Meyer, Phys. Rev. D **101**, 074515 (2020), [arXiv:2003.04177].

[25] G. Wang *et al.* (χQCD), Phys. Rev. D **107**, 3, 034513 (2023), [arXiv:2204.01280].

[26] C. Aubin *et al.*, Phys. Rev. D **106**, 5, 054503 (2022), [arXiv:2204.12256].

[27] M. Cè *et al.*, Phys. Rev. D **106**, 11, 114502 (2022), [arXiv:2206.06582].

[28] C. Alexandrou *et al.* (ETM), Phys. Rev. D **107**, 7, 074506 (2023), [arXiv:2206.15084].

[29] T. Blum *et al.* (RBC, UKQCD), Phys. Rev. D **108**, 5, 054507 (2023), [arXiv:2301.08696].

[30] S. Kuberski *et al.*, JHEP **03**, 172 (2024), [arXiv:2401.11895].

[31] A. Boccaletti *et al.* (2024), [arXiv:2407.10913].

[32] S. Spiegel and C. Lehner, Phys. Rev. D **111**, 11, 114517 (2025), [arXiv:2410.17053].

[33] T. Blum *et al.* (RBC, UKQCD), Phys. Rev. Lett. **134**, 20, 201901 (2025), [arXiv:2410.20590].

[34] D. Djukanovic *et al.*, JHEP **04**, 098 (2025), [arXiv:2411.07969].

[35] C. Alexandrou *et al.* (ETM), Phys. Rev. D **111**, 5, 054502 (2025), [arXiv:2411.08852].

[36] A. Bazavov *et al.* (Fermilab Lattice, HPQCD, MILC), Phys. Rev. D **111**, 9, 094508 (2025), [arXiv:2411.09656].

[37] A. Bazavov *et al.* (Fermilab Lattice, HPQCD, MILC), Phys. Rev. Lett. **135**, 1, 011901 (2025), [arXiv:2412.18491].

[38] A. Keshavarzi, D. Nomura and T. Teubner, Phys. Rev. D **101**, 014029 (2020), [arXiv:1911.00367].

[39] L. Di Luzio *et al.*, Phys. Rev. Lett. **134**, 1, 011902 (2025), [arXiv:2408.01123].

[40] A. Kurz *et al.*, Phys. Lett. B **734**, 144 (2014), [arXiv:1403.6400].

[41] G. Colangelo *et al.*, JHEP **09**, 074 (2015), [arXiv:1506.01386].

[42] P. Masjuan and P. Sánchez-Puertas, Phys. Rev. D **95**, 5, 054026 (2017), [arXiv:1701.05829].

[43] G. Colangelo *et al.*, JHEP **04**, 161 (2017), [arXiv:1702.07347].

[44] M. Hoferichter *et al.*, JHEP **10**, 141 (2018), [arXiv:1808.04823].

[45] G. Eichmann *et al.*, Phys. Lett. B **797**, 134855 (2019), [Erratum: Phys. Lett. B **799**, 135029 (2019)], [arXiv:1903.10844].

[46] J. Bijnens, N. Hermansson-Truedsson and A. Rodríguez-Sánchez, Phys. Lett. B **798**, 134994 (2019), [arXiv:1908.03331].

[47] J. Leutgeb and A. Rebhan, Phys. Rev. D **101**, 11, 114015 (2020), [arXiv:1912.01596].

[48] L. Cappiello *et al.*, Phys. Rev. D **102**, 1, 016009 (2020), [arXiv:1912.02779].

[49] P. Masjuan, P. Roig and P. Sánchez-Puertas, J. Phys. G **49**, 1, 015002 (2022), [arXiv:2005.11761].

[50] J. Bijnens *et al.*, JHEP **10**, 203 (2020), [arXiv:2008.13487].

[51] J. Bijnens *et al.*, JHEP **04**, 240 (2021), [arXiv:2101.09169].

[52] I. Danilkin, M. Hoferichter and P. Stoffer, Phys. Lett. B **820**, 136502 (2021), [arXiv:2105.01666].

[53] D. Stamen *et al.*, Eur. Phys. J. C **82**, 5, 432 (2022), [arXiv:2202.11106].

[54] J. Leutgeb, J. Mager and A. Rebhan, Phys. Rev. D **107**, 5, 054021 (2023), [arXiv:2211.16562].

[55] M. Hoferichter, B. Kubis and M. Zanke, JHEP **08**, 209 (2023), [arXiv:2307.14413].

[56] M. Hoferichter, P. Stoffer and M. Zillinger, JHEP **04**, 092 (2024), [arXiv:2402.14060].

[57] E. J. Estrada *et al.*, JHEP **12**, 203 (2024), [arXiv:2409.10503].

[58] O. Deineka, I. Danilkin and M. Vanderhaeghen, Phys. Rev. D **111**, 3, 034009 (2025), [arXiv:2410.12894].

[59] G. Eichmann *et al.*, Eur. Phys. J. C **85**, 4, 445 (2025), [arXiv:2411.05652].

[60] J. Bijnens, N. Hermansson-Truedsson and A. Rodríguez-Sánchez, JHEP **03**, 094 (2025), [arXiv:2411.09578].

[61] M. Hoferichter, P. Stoffer and M. Zillinger, JHEP **02**, 121 (2025), [arXiv:2412.00178].

[62] S. Holz *et al.*, JHEP **04**, 147 (2025), [arXiv:2412.16281].

[63] L. Cappiello *et al.*, JHEP **07**, 033 (2025), [arXiv:2501.09699].

[64] G. Colangelo *et al.*, Phys. Lett. B **735**, 90 (2014), [arXiv:1403.7512].

[65] T. Blum *et al.*, Phys. Rev. Lett. **124**, 13, 132002 (2020), [arXiv:1911.08123].

[66] E.-H. Chao *et al.*, Eur. Phys. J. C **81**, 7, 651 (2021), [arXiv:2104.02632].

[67] E.-H. Chao *et al.*, Eur. Phys. J. C **82**, 8, 664 (2022), [arXiv:2204.08844].

[68] T. Blum *et al.* (RBC, UKQCD), Phys. Rev. D **111**, 1, 014501 (2025), [arXiv:2304.04423].

[69] Z. Fodor *et al.*, Phys. Rev. D **111**, 11, 114509 (2025), [arXiv:2411.11719].

[70] H. R. P. Ferguson and D. H. Bailey, Technical report, RNR-91-032 (1992), URL `https://www.davidhbailey.com/dhbpapers/pslq.pdf`.

[71] J. Bailey *et al.* (CERN-Mainz-Daresbury), Nucl. Phys. B **150**, 1 (1979).

[72] H. N. Brown *et al.* (Muon $g-2$), Phys. Rev. Lett. **86**, 2227 (2001), [hep-ex/0102017].

[73] G. W. Bennett *et al.* (Muon $g-2$), Phys. Rev. Lett. **89**, 101804 (2002), [Erratum: Phys. Rev. Lett. **89**, 129903 (2002)], [hep-ex/0208001].

[74] G. W. Bennett *et al.* (Muon $g-2$), Phys. Rev. Lett. **92**, 161802 (2004), [hep-ex/0401008].

[75] P. J. Mohr *et al.*, Rev. Mod. Phys. **97**, 2, 025002 (2025), [arXiv:2409.03787].

[76] G. T. Danby *et al.*, Nucl. Instrum. Meth. A **457**, 151 (2001).

[77] A. P. Schreckenberger *et al.*, Nucl. Instrum. Meth. A **1011**, 165597 (2021), [arXiv:2104.07805].

[78] V. Bargmann, L. Michel and V. L. Telegdi, Phys. Rev. Lett. **2**, 435 (1959).

[79] M. Abe *et al.*, PTEP **2019**, 5, 053C02 (2019), [arXiv:1901.03047].

[80] D. Flay *et al.*, JINST **16**, 12, P12041 (2021), [arXiv:2109.08992].

[81] M. Farooq *et al.*, Phys. Rev. Lett. **124**, 22, 223001 (2020).

[82] S. Corrodi *et al.* (Muon $g-2$), JINST **15**, 11, P11008 (2020), [arXiv:2003.06244].

[83] E. Swanson *et al.*, Nucl. Instrum. Meth. A **1075**, 170338 (2025), [arXiv:2410.08279].

[84] B. T. King *et al.*, JINST **17**, 02, P02035 (2022), [arXiv:2111.02076].

[85] K. S. Khaw *et al.* (Muon $g-2$), Nucl. Instrum. Meth. A **945**, 162558 (2019), [arXiv:1905.04407].

[86] O. Kim *et al.*, New J. Phys. **22**, 6, 063002 (2020), [arXiv:1902.02959].

[87] T. Aoyama *et al.*, Phys. Rept. **887**, 1 (2020), [arXiv:2006.04822].

[88] Muon $g-2$ Theory Initiative `https://muon-gm2-theory.illinois.edu/`.

[89] J. S. Schwinger, Phys. Rev. **73**, 416 (1948).

[90] A. Petermann, Helv. Phys. Acta **30**, 407 (1957).

[91] C. M. Sommerfield, Ann. Phys. (N.Y.) **5**, 26 (1958).

[92] S. Laporta and E. Remiddi, Phys. Lett. B **379**, 283 (1996), [hep-ph/9602417].

[93] H. H. Elend, Phys. Lett. **20**, 682 (1966), [Erratum: Phys. Lett. **21**, 720 (1966)].

[94] S. Laporta and E. Remiddi, Phys. Lett. B **301**, 440 (1993).

[95] S. Laporta, Nuovo Cim. A **106**, 675 (1993).

[96] S. Laporta, Phys. Lett. B **772**, 232 (2017), [arXiv:1704.06996].

[97] T. Kinoshita and M. Nio, Phys. Rev. D **73**, 013003 (2006), [hep-ph/0507249].

[98] R. Jackiw and S. Weinberg, Phys. Rev. D **5**, 2396 (1972).

[99] I. Bars and M. Yoshimura, Phys. Rev. D **6**, 374 (1972).

[100] G. Altarelli, N. Cabibbo and L. Maiani, Phys. Lett. B **40**, 415 (1972).

[101] W. A. Bardeen, R. Gastmans and B. E. Lautrup, Nucl. Phys. B **46**, 319 (1972).

[102] K. Fujikawa, B. Lee and A. Sanda, Phys. Rev. D **6**, 2923 (1972).

[103] V. Tishchenko *et al.* (MuLan), Phys. Rev. D **87**, 5, 052003 (2013), [arXiv:1211.0960].

[104] A. Czarnecki, B. Krause and W. J. Marciano, Phys. Rev. Lett. **76**, 3267 (1996), [hep-ph/9512369].

[105] S. Heinemeyer, D. Stöckinger and G. Weiglein, Nucl. Phys. B **699**, 103 (2004), [hep-ph/0405255].

[106] T. Gribouk and A. Czarnecki, Phys. Rev. D **72**, 053016 (2005), [hep-ph/0509205].

[107] A. Czarnecki, B. Krause and W. J. Marciano, Phys. Rev. D **52**, 2619 (1995), [hep-ph/9506256].

[108] S. Peris, M. Perrottet and E. de Rafael, Phys. Lett. B **355**, 523 (1995), [hep-ph/9505405].

[109] M. Knecht *et al.*, JHEP **11**, 003 (2002), [hep-ph/0205102].

[110] K. Melnikov, Phys. Lett. B **639**, 294 (2006), [hep-ph/0604205].

[111] M. Cè *et al.*, JHEP **08**, 220 (2022), [arXiv:2203.08676].

[112] G. Degrassi and G. Giudice, Phys. Rev. D **58**, 053007 (1998), [hep-ph/9803384].

[113] M. Hoferichter, P. Stoffer and M. Zillinger, Phys. Rev. Lett. **134**, 6, 061902 (2025), [arXiv:2412.00190].

[114] C. Bouchiat and L. Michel, J. Phys. Radium **22**, 2, 121 (1961).

[115] S. J. Brodsky and E. de Rafael, Phys. Rev. **168**, 1620 (1968).

[116] M. N. Achasov *et al.* (SND), J. Exp. Theor. Phys. **103**, 380 (2006), [Zh. Eksp. Teor. Fiz. **130**, 437 (2006)], [hep-ex/0605013].

[117] R. R. Akhmetshin *et al.* (CMD-2), Phys. Lett. B **648**, 28 (2007), [hep-ex/0610021].

[118] J. P. Lees *et al.* (BaBar), Phys. Rev. D **86**, 032013 (2012), [arXiv:1205.2228].

[119] A. Anastasi *et al.* (KLOE-2), JHEP **03**, 173 (2018), [arXiv:1711.03085].

[120] M. Ablikim *et al.* (BESIII), Phys. Lett. B **753**, 629 (2016), [Erratum: Phys. Lett. B **812**, 135982 (2021)], [arXiv:1507.08188].

[121] M. Davier *et al.*, Eur. Phys. J. C **77**, 12, 827 (2017), [arXiv:1706.09436].

[122] A. Keshavarzi, D. Nomura and T. Teubner, Phys. Rev. D **97**, 11, 114025 (2018), [arXiv:1802.02995].

[123] G. Colangelo, M. Hoferichter and P. Stoffer, JHEP **02**, 006 (2019), [arXiv:1810.00007].

[124] M. Hoferichter, B.-L. Hoid and B. Kubis, JHEP **08**, 137 (2019), [arXiv:1907.01556].

[125] M. Davier *et al.*, Eur. Phys. J. C **80**, 3, 241 (2020), [Erratum: Eur. Phys. J. C **80**, 410 (2020)], [arXiv:1908.00921].

[126] G. Colangelo *et al.*, JHEP **10**, 032 (2022), [arXiv:2208.08993].

[127] P. Stoffer, G. Colangelo and M. Hoferichter, JINST **18**, 10, C10021 (2023), [arXiv:2308.04217].

[128] T. P. Leplumey and P. Stoffer (2025), [arXiv:2501.09643v1].

[129] M. Davier *et al.*, Eur. Phys. J. C **84**, 7, 721 (2024), [arXiv:2312.02053].

[130] A. Keshavarzi *et al.*, Phys. Rev. D **111**, 1, L011901 (2025), [arXiv:2409.02827].

[131] M. N. Achasov *et al.* (SND), JHEP **01**, 113 (2021), [arXiv:2004.00263].

[132] F. V. Ignatov *et al.* (CMD-3), Phys. Rev. D **109**, 11, 112002 (2024), [arXiv:2302.08834].

[133] F. V. Ignatov *et al.* (CMD-3), Phys. Rev. Lett. **132**, 23, 231903 (2024), [arXiv:2309.12910].

[134] J. Calmet *et al.*, Phys. Lett. **61B**, 283 (1976).

[135] M. Hoferichter and T. Teubner, Phys. Rev. Lett. **128**, 11, 112002 (2022), [arXiv:2112.06929].

[136] R. Alemany, M. Davier and A. Hoecker, Eur. Phys. J. C **2**, 123 (1998), [hep-ph/9703220].

[137] V. Cirigliano, G. Ecker and H. Neufeld, Phys. Lett. B **513**, 361 (2001), [hep-ph/0104267].

[138] V. Cirigliano, G. Ecker and H. Neufeld, JHEP **08**, 002 (2002), [hep-ph/0207310].

[139] F. Flores-Báez *et al.*, Phys. Rev. D **74**, 071301 (2006), [hep-ph/0608084].

[140] M. Davier *et al.*, Eur. Phys. J. C **66**, 127 (2010), [arXiv:0906.5443].

[141] J. A. Miranda and P. Roig, Phys. Rev. D **102**, 114017 (2020), [arXiv:2007.11019].

[142] G. López Castro, A. Miranda and P. Roig, Phys. Rev. D **111**, 7, 073004 (2025), [arXiv:2411.07696].

[143] M. Hoferichter *et al.*, Phys. Rev. Lett. **131**, 16, 161905 (2023), [arXiv:2307.02532].

[144] D. Bernecker and H. B. Meyer, Eur. Phys. J. A **47**, 148 (2011), [arXiv:1107.4388].

[145] G. Colangelo *et al.* (2022), [arXiv:2203.15810].

[146] F. Campanario *et al.*, Phys. Rev. D **100**, 7, 076004 (2019), [arXiv:1903.10197].

[147] F. Ignatov and R. N. Lee, Phys. Lett. B **833**, 137283 (2022), [arXiv:2204.12235].

[148] G. Colangelo *et al.*, JHEP **08**, 295 (2022), [Erratum: JHEP **03**, 217 (2025)], [arXiv:2207.03495].

[149] G. Abbiendi *et al.* (2022), [arXiv:2201.12102].

[150] J. P. Lees *et al.* (BaBar), Phys. Rev. D **108**, 11, L111103 (2023), [arXiv:2308.05233].

[151] E. Budassi *et al.*, JHEP **05**, 196 (2025), [arXiv:2409.03469].

[152] R. Aliberti *et al.*, SciPost Phys. Comm. Rep. **9**, 1 (2025), [arXiv:2410.22882].
[153] C. M. Carloni Calame *et al.*, Phys. Lett. B **746**, 325 (2015), [arXiv:1504.02228].
[154] G. Abbiendi *et al.* (MUonE), Eur. Phys. J. C **77**, 3, 139 (2017), [arXiv:1609.08987].
[155] P. Banerjee *et al.*, Eur. Phys. J. C **80**, 6, 591 (2020), [arXiv:2004.13663].